Microgrid Losses: When the Whole is Greater Than the Sum of Its Parts

Maxim Buevich † Xiao Zhang † Oliver Shih † Dan Schnitzer ‡
Tristan Escalada ‡ Arthur Jacquiau-Chamski ‡ Jon Thacker ‡ Anthony Rowe †
† Electrical and Computer Engineering Department, Carnegie Mellon University
‡ SparkMeter Inc.
{mbuevich,xiaozhan,oshih,agr}@andrew.cmu.edu
{dan,tristan,arthur,jon}@sparkmeter.io

ABSTRACT

Non-Technical Loss (NTL) represents a major challenge when providing reliable electrical service in developing countries, where it often accounts for 11-15% of total generation capacity [1]. NTL is caused by a variety of factors such as theft, unmetered homes, and inability to pay, which at volume can lead to system instability, grid failure, and major financial losses for providers.

In this paper, we investigate error sources and techniques for separating NTL from total losses in microgrids. We adopt and compare two classes of approaches for detecting NTL: (1) model-driven and (2) data-driven. The model-driven class considers the primary sources of state uncertainty including line losses, meter consumption, meter calibration error, packet loss, and sample synchronization error. In the data-driven class, we use two approaches that learn grid state based on training data. The first approach uses a regression technique on an NTL-free period of grid operation to capture the relationship between state error and total consumption. The second approach uses an SVM trained on synthetic NTL data. Both classes of approaches can provide a confidence interval based on the amount of detected NTL. We experimentally evaluate and compare the approaches on wireless meter data collected from a 525-home microgrid deployed in Les Anglais, Haiti. We see that both are quite effective, but that the data-driven class is significantly easier to implement. In both cases, we are able to experimentally evaluate to what degree we can reliably separate NTL from total losses.

Permission to make digital or hard copies of all or part of this work for personal or classroom use is granted without fee provided that copies are not made or distributed for profit or commercial advantage and that copies bear this notice and the full citation on the first page. To copy otherwise, to republish, to post on servers or to redistribute to lists, requires prior specific permission and/or a fee.
Copyright 200X ACM X-XXXXX-XX-X/XX/XX ...$5.00.

Keywords

Microgrid, NTL Detection

1. INTRODUCTION

As reported by the World Bank Group in 2011 [1], Non-Technical Loss (NTL) accounts for 15% of total generation capacity in the Latin America & Caribbean market and 11% in the Sub-Saharan Africa markets. Together with corruption and weak regulatory environments, NTL are a major contributor to the poor state of operations of utilities in developing countries [2]. NTL prevents utilities from achieving cost recovery because they cannot fully pay for the cost of energy generated. This leads to a vicious cycle: inability to pay for generation results in supply shortages that cause outages; outages result in customer dissatisfaction, so even customers who were paying for electricity may be less inclined to do so and may self-generate rather than purchase electricity from the utility; a smaller customer base results in even lower tariff collection, and then even greater supply shortages.

Utilities would benefit greatly from being able to locate NTL and address the problem with consumers directly. Smart metering enables utilities to do this on a real-time basis, whereas conventional metering systems provide utilities with only a monthly resolution.

Theft is a large component of NTL on both central and remote microgrids [3]. Most often, theft is carried out by making an unauthorized connection to the microgrid distribution line. In other cases, theft is carried out by authorized customers who bypass their meters. Monitoring theft is therefore difficult, especially on systems that serve a few hundred households. Theft is most often dealt with through strong local institutions that can impose a credible threat of penalty. However, penalties are often unenforced, and theft persists on many systems due to lack of visibility into losses.

In this paper, we discuss the detection of NTL in a rural microgrid deployment in Les Anglais (LA), Haiti. An

initial version of the microgrid was first described in [4], which included wireless energy meters on 54 homes. The system utilized excess capacity from a diesel generator powering a local cellular tower. Over the last year, we have updated the microgrid with a commercial version of the system developed by SparkMeter Inc. The grid now services more than 525 homes powered by a 93kW solar PV array with 400kWh of battery capacity and an auxiliary diesel backup generator. We use detailed characteristics of the distribution network, communication network and data traces collected from the microgrid to compare and contrast three NTL approaches. The first is a model-driven approach that estimates losses using an Optimal Power Flow (OPF) simulator based on detailed grid topology, shown in Figure 1. The second approach uses a regression model that is trained on an initial data collection period. The third approach is SVM-based and is trained on synthetic NTL data.

One of the novel features of our underlying system is the use of time synchronized sampling of power data across the network to aid in separating NTL from total losses. We determine the state of the microgrid system by comparing all of our meter readings with a set of totalizers (aggregators) installed at each generation source. Ideally, the sum of the loads should match the generation. However, there are multiple sources of error including (1) line losses, (2) metering error, (3) meter consumption, (4) temporal meter sampling jitter, and (5) packet loss. We define this difference as the grid's *State Error*. Using real-world data collected from the network, we explore the magnitude and implications of each of these sources of error. We see that if available, detailed modeling information (with some tuning based on empirical data) is able to slightly outperform our data-driven-only based detectors. However, the data driven detectors are significantly easier to configure and maintain with a level of performance that can still yield action-able suggestions about when NTL occurs and how much energy is missing.

2. RELATED WORK

Microgrids are typically developed by governments agencies, private developers and NGOs as a means to provide access to electricity in areas of the world where it is financially, physically or institutionally difficult to extend the reach of the central grid [3]. Microgrid deployments range in scale and complexity from small deployments such as DESI Power's four village microgrids in Bihar, India powered by biomass gasification [5] to the West Bengal Renewable Energy Development Agency's 18 microgrids powered primarily by solar PV in the Sundarbans [6] to Nepal, which powers 59,000 households with over 300 micro-hydro systems [7]. These grids also vary substantially in the services they provide.

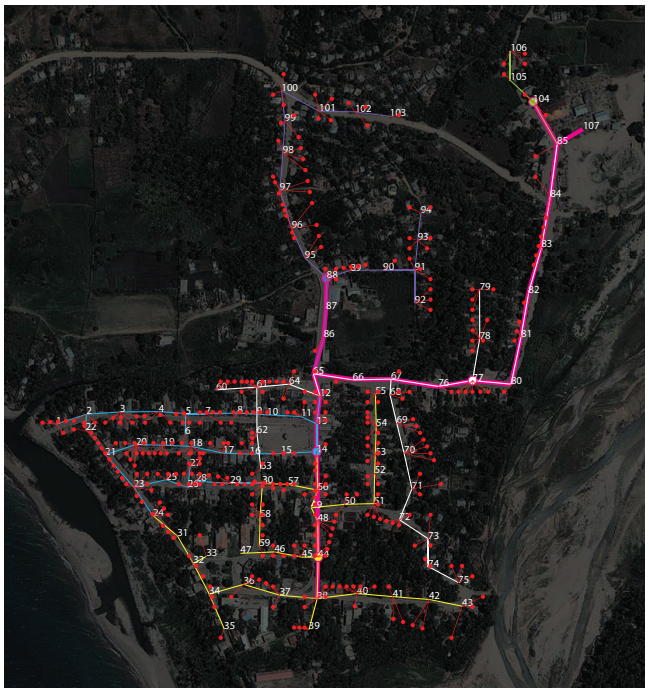

Figure 1: Les Anglais microgrid topology

Some microgrids are designed to provide only the most basic energy services, such as lighting in the evening, while others are designed to power cold storage and other productive commercial or agricultural loads such as mills and irrigation pumps [8].

Modern microgrid developers are turning to advanced low-cost pre-paid meters to solve problems of customer over-use and poor tariff collection. Companies such as Devergy [9], Circutor [10], Inensus [11], Powerhive [12] and Gram Power [13] have each developed such metering systems targeted at microgrids serving low-income customers. Even in their early stages, these systems offer significant advantages over both conventional metering systems and less sophisticated pre-paid meters such as those made by Conlog [14]. Those advantages include greater flexibility in billing, remote system monitoring, price-responsive DSM, load-shedding, and dynamic power- and energy-limiting [15].

Unfortunately, many microgrids fall into non-functioning states due to any one of a number of factors, including low levels of tariff collection, poor maintenance, customer over-usage (which causes brown-outs), and unmet growth in demand [3]. Attempts at modeling microgrid operations have shown that a number of interventions can improve microgrid sustainability, such as the use of renewable energy to improve cost-effectiveness [16] [17] [18], energy efficiency [18], and the use of demand side management (DSM) strategies and technologies [15] [19]. However, NTL still stands as a factor that drasti-

Figure 2: Solar PV array with battery and diesel generation (left) and Sparkmeter hardware (right)

cally hinders all of these efforts. In this paper, we look holistically at separation of NTL from total losses given a model of the grid, its metering characteristics, and the communication network used to collect data.

There have been multiple techniques proposed to detect and even actively thwart non-technical loss that range from policy to technical engineering methods. In [20], the authors provide a rigorous analysis of the different types of NTL and various existing solutions. Some of the most common technical methods involve designing tamper resistant meters and per-user trending of consumption data over time. Managerial methods include periodic line inspection and surveillance. [21] discusses installing filters into smart meters and then injecting destructive harmonics into the line that would destroy any illegally attached appliances. [22] proposes a similar approach to our approach where meter readings at branches within a distribution tree are aggregated and compared in order to find power theft. The work is proposed as a concept without any technical explanation or evaluation. In [23], the authors propose an optimal state-estimation approach for theft detection. This approach compares consumption with aggregators and attempts to identify theft as a measurement bias. While promising, the work is conducted entire in simulation and not evaluated on real data. As we see in our real deployment, some of the assumptions often applied when modeling a grid are either hard to capture or fail to be accurate in practice.

There have also been a number of efforts that use data mining and machine learning in an attempt to classify non-technical loss. [24, 25] use Support Vector Machines (SVM) based on historical data and Genetic Algorithms to identify abnormal patterns. These approaches often fail in practice for two main reasons: (1) microgrids naturally scale in size over time and (2) theft from the grid is usually comprised of similar appliances as those found in legally paying homes making individual signatures nearly identical. In [26], the authors use a combination of network security, on meter tamper resistance and non-intrusive load monitoring (NILM) to detect theft. This approach looks at patterns in appliance on and off transitions over time in order to detect anomalous behavior. While promising, this approach assumes an accurate NILM approach that is still difficult to achieve in practice.

A project from The Impact Lab and Jamaica Public Service (JPS) takes a machine learning approach for detecting customer NTL by identifying changes in individual home usage patterns over time [27]. Their goal is to detect drops in consumption that would be indicative of offloading appliances to unmetered lines. They train a random decision forest classifier on individual 15 minute data collected per home. This approach shows great promise and can be used in conjunction with our proposed methods to not only detect NTL, but possibly localize likely areas in the grid. Unlike approaches that have access to totalizer data, the JPS approach is unable to detect new NTL that is not simply offloading from an existing metered home.

3. LES ANGLAIS MICROGRID

Figure 2 shows photos of the updated grid generation, as well as a picture of the Sparkmeter energy meter installed on a home. As previously mentioned, the latest grid installation is comprised of 525 homes that are powered from a 93kW solar PV array, 400 kWh of battery capacity and a small diesel backup generator. The topology of the LA grid is shown in Figure 1, in which different colors represent different subdivisions: the thick (pink) lines represent the three-phase Medium Voltage (MV) lines with a nominal voltage of 7.2kV. The other subdivisions are single-phase Low Voltage (LV) lines with a nominal voltage of 120V. The LV subdivisions are connected to the MV lines via split-phase transformers and to individual houses via service drops. There are three totalizer meters that collect aggregate metering data for each of the three subdivisions powered

by each phase in the distribution system. The location of each home was collected using GPS.

In total, there are 1102 meters of MV wiring in the grid with relatively negligible loss given their low gauge and high voltage. The LV lines, having an AWG of 2 and a total combined length of 4210 meters which accounts for the primary source of line loss. There are also three transformers responsible for converting the MV to LV. Typically, in a microgrid, approximately one-third of loss is found in transformers and the rest in wiring.

The microgrid has been operating continuously for more than 12 months. All of the meter readings are synchronized and accompanied by logs of wireless communication traffic along with a detailed description of the physical grid topology. The full network reports data from 525 homes every 15 minutes with each meter sampling globally within approximately 10 milliseconds. Figure 3 shows an example of the power consumed over time of one home as well as the entire grid.

3.1 Synchronous Sampling

Meters communicate with a gateway responsible for collecting data wirelessly using a proprietary protocol built on IEEE 802.15.4. The network provides mesh communication and time-synchronized sampling. The protocol allows full control over network addressing and route selection from the gateway while delivering a consistent notion of time across the network. The gateway individually polls each meter sequentially, updating status information and requesting data. All requests are either routed or flooded across the network. Each request from the gateway carries with it the current network time and the synchronous sampling interval (or heartbeat). At the moment of each heartbeat, all meters will record the average power, voltage and current of the previous heartbeat period. Additionally the energy, frequency, power factor and instantaneous power are recorded for this exact moment in time. The network maintains highly reliable synchronous sampling by including the timing information in every outbound packet from the gateway which can be overheard by any

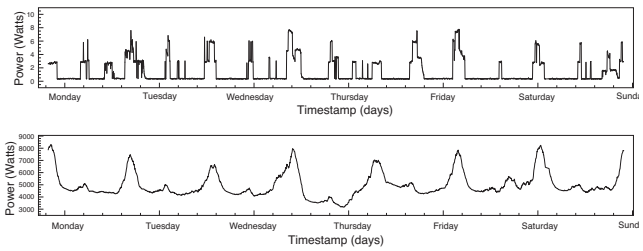

Figure 3: Example power trace over a week for a single house (top) and entire grid (bottom)

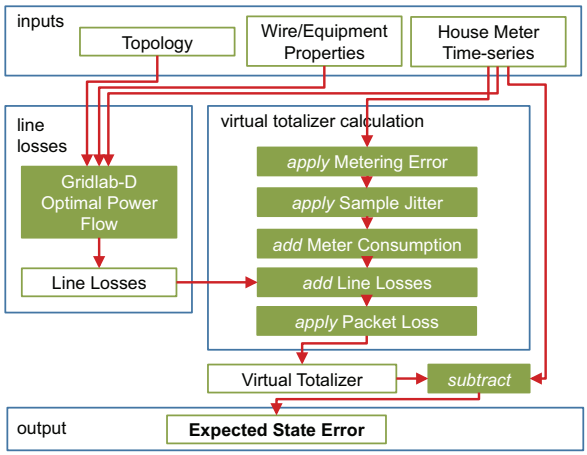

Figure 4: Microgrid modeling workflow

node. Timing data is adjusted on each hop across the network to account for hop-delay. Testbed evaluations indicate that the global heart-beat is accurate to below 5ms.

4. COMPONENTS OF STATE ERROR

Our microgrid model relies on accurate topology information, power readings from individual meters, and the properties of wiring and equipment. These are used to calculate the expected state error, the difference in total power readings at the generation and the loads. State error is made up of multiple components, each of which must themselves be modeled. Figure 4 shows the workflow by which state error is calculated. The inputs are fed into Gridlab-D, which performs an Optimal Power Flow simulation to calculate line and transformer losses. These losses and the house meter readings are then used in a process which models the remaining components of state error to generate a virtual totalizer power reading. Finally, subtracting from the totalizer reading the sum of all house meter readings yields an expected state error. The following sections describe in detail how the components of state error are modeled.

4.1 Line Losses

We employ GridLAB-D as the engine to calculate the power flow as well as our line loss statistics, using the topology of the LA grid (i.e. how the houses, power lines, service drops are connected to one another) as an input. The power line traces are captured from an annotated satellite photo; the wire properties are derived from the vendor data sheets; the pole locations are obtained from the project records; the house locations are imported from the GPS log. Our model assumes that houses are connected to the nearest utility pole. While

this is not true for every house on the physical grid, it is an adequate approximation for the purpose of simulation. With this topology information, as well as the synchronized measurement at each timestamp, we are able to generate a GridLAB-D input file (.glm) that models the instantaneous LA power grid. Next, GridLAB-D calculates the power flow for that timestamp and saves the results into an XML file. Finally, the XML file is analyzed to give us the line loss summary and powerflow at each node in the grid.

In order to understand the impact of line loss on energy NTL detection, the power flows of the LA grid are simulated under multiple loading scenarios, with the assumption of nominal line voltages. We simulate multiple loading scenarios while varying the number of houses connected to the grid. The first scenario represents the current LA grid, where there are over 400 houses connected by 6835 meters of service drops; the second scenario restricts the number of houses connected at each pole to be smaller or equal to 3, where 272 houses are connected by 4631 meters of service drops; the last scenario is the case that each pole can only connect 1 house, where there are 104 houses and the length of service drops is 1886 meters in total.

The power flows for the scenarios described above are simulated every 15 minutes for 24 hours - there are 96 simulations for each scenario. The line loss and the total load in the grid for each of these simulations are plotted in Figure 5, where each point stands for a simulation. From the plot, we observe that (1) the more houses connected in the grid, the higher the percentage of line loss to the total load; (2) under the same configuration, the relationship between line loss and the total load appears exponential.

4.2 Metering Error and Meter Consumption

Metering standards like IEC 61036 specify multiple classes of meter accuracies that can range from 0.2% to 2.5% in terms of maximum error at a given power factor. After calibration, we see our meters generally exhibit Gaussian error. In the LA grid, each meter is 2.0% accurate with a typical load limit of 30 W. At maximum load each house would expect to see 0.6 W of error. Assuming a summation of Gaussian distributions, the magnitude of the noise will grow as the root mean square of the total which is relatively small even for a large number of nodes. For this reason, the aggregator's error is critical in that it has a larger impact than the distributed meters and it directly bounds the system's ability to detect NTL.

The meters themselves have an average power consumption of 2.0 Watts, which remains stable over time. The meters do not account for their own power consumption, however, their consumption is reflected in totalizer power readings because totalizers are installed at points of generation. The house meter consumption thus manifests as a constant positive component of state error which must be accounted for.

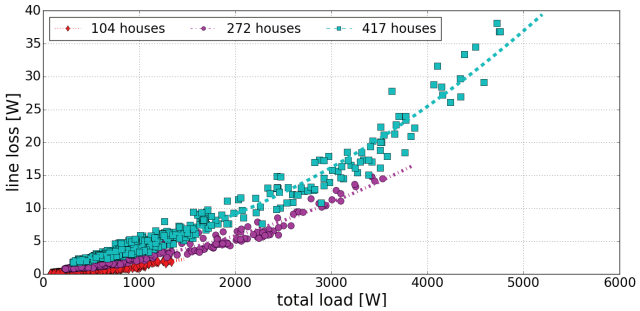

Figure 5: Simulated trace-based aggregate line loss

4.3 Meter Sampling Jitter

Our method of NTL detection is fundamentally based on comparing a single sample taken by a totalizer and a summation of many distributed samples taken by wireless meters. In such a scheme, the times at which the meter samples were taken can have a significant effect on the final result. In order to understand this, we quantify the impact that this sampling jitter has on the state error calculation.

In the first stage of the LA microgrid deployment, there was a period of a few weeks when data from 48 houses was being collected at 1Hz. We use this high-speed data to extrapolate what would happen as the jitter in sensor sampling increased. Figure 6 shows the results of a state error simulation which contains a controlled amount of sampling jitter and no other sources of error. Instead of being perfectly synchronized, meter samples are randomly selected (with a uniform distribution) from inside a synthetic jitter window, which has a

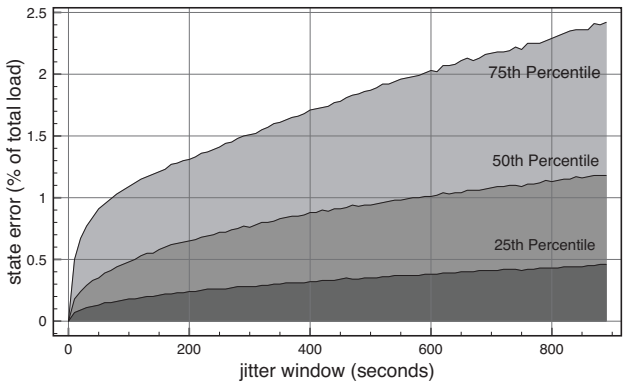

Figure 6: Impact of jitter on state error

width measured in seconds. As the jitter window is increased, the samples are de-synchronized. For instance, in Figure 6 we see that when sampling within a 30-second jitter window, the median state error is 0.29%; whereas, sampling within a 15-minute window, which is done by most conventional meters, results in a median state error of 1.18%.

4.4 Packet Loss

Lost meter packets play an important role in measuring the state of the system. If a meter does not report a value in a particular cycle, there are numerous error correction options including: (1) ignore the sampling period, (2) use a previous value for the dropped reading, (3) predict the value based on a model or (4) assume the worst-case consumption of the missing meter. For example, if a single meter value is missing we must increase our tolerance for detecting NTL by the expected consumption in that home during the period. Many missing meter readings compounds the problem.

In the LA microgrid, over 72 days with a 15 minute period, 94.03% of the meter polling periods returned all of the meter values. Note that the gateway continuously polls any missing meters until the start of the next period allowing for ample low-level retry opportunities (overall packet reception rate was >99.6%). Figure 7 shows the packet distributions associated with the network failure cases. The top graph shows how often consecutive periods failed to collect data from all meters. For example, there were 21 cases where the dropped data was only for a single period (15 minutes), 14 cases where it continued for two periods (30 minutes), and so on. The three large blackouts were due to scheduled grid maintenance. The bottom graph in Figure 7 shows the distribution of how many meters would fail to reply given a period that includes dropped messages. We see that most drops include only a few meters, but there are occasions when large areas of the network are unreachable. Given the reliability of the network and, we adopt a scheme which ignores polling cycles with missing meter readings. In practice this seems sufficient, and could easily be improved with the use of previous values to replace missing data points.

5. NTL DETECTORS

In this section, we build on our model of microgrid losses by using it to implement a model-driven NTL detector. We also propose two data-driven detectors which, in contrast, rely on a training period. Both classes of detectors are based on state error, the mismatch between total energy seen by the meters and the total energy seen by the totalizers. The detectors use separate methods to calculate a detection threshold, which is compared with state error to identify NTL.

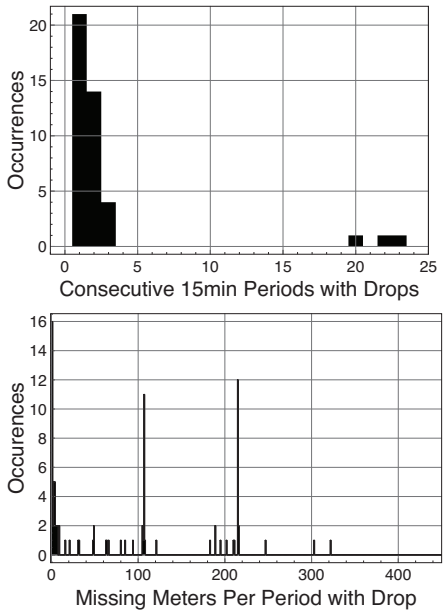

Figure 7: Network packet loss

5.1 Model-driven Detection

The model-driven detector identifies NTL by comparing state error with a threshold derived from the microgrid loss model. The threshold combines expected line-losses with a pre-defined buffer consisting of multiple other components. Calculations are made based on instantaneous true power, which is sampled at all meters simultaneously. Because the meter firmware was designed around a TDMA network protocol which maintains millisecond-level time and implements synchronous sampling, it was not necessary to incorporate meter sampling jitter into the model-driven detector. Packet loss after link-level retries was also found to be negligible in the real-world deployment, thus the few instances of packet loss were safely ignored without affecting the final results.

For a value of time t, the value of the detector threshold in Watts is given by

$$d_m(t) = m + l(t) + u$$

where m is the average combined power consumption of the meters, $l(t)$ is the line losses at time t, and u is a user-specified margin. The power consumption of the meters is captured by the totalizers but not by the meters themselves, and thus adds to the state error. Line losses are time-varying and depend not only on line properties but also the magnitudes and locations of all loads in the microgrid. The user-specified margin can be chosen based on the desired sensitivity and specificity of detection.

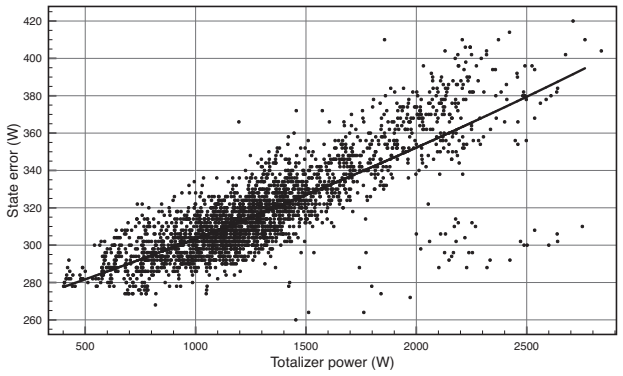

Figure 8: Regression model of state error

5.2 Regression Detector

Much like the model-driven detector, the regression-based detector compares state error with a threshold to identify NTL. However, this detector does not incorporate any grid-topology-specific modeling in its calculations. The regression-based detector is based on an exponential regression, shown in Figure 8, that captures the relationship between power consumption measured by the totalizer at a point in time and the state error at the same point in time. For accurate detection, the shape of the detector must be learned by calculating the regression from past data that does not contain NTL. The detector threshold is then equal to the regression, with the addition of a constant buffer based on the state error deviation from the regression line.

For a given value of power P, the value of the data-driven detector threshold is given by

$$d_r(P) = a * e^{b*P} + c$$

where a and b are the regression variables and c is the value of the constant buffer. The buffer is calculated from the distibution of state error around the regression line, shown in Figure 9. In practice, we found that a buffer equal to the 2-sigma deviation of state error is appropriate for NTL detection.

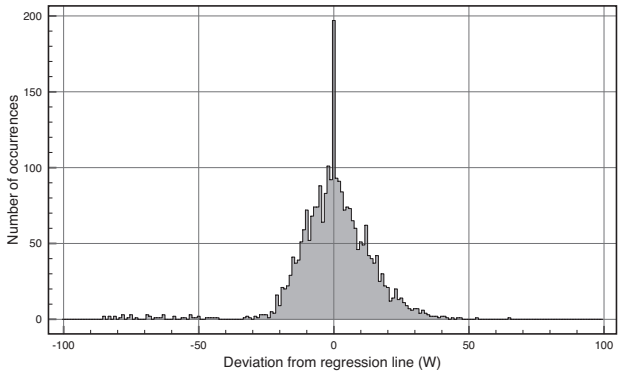

Figure 9: Histogram of state error deviation from regression

5.3 SVM Detector

In the previous regression model, we attempt to model the typical distribution of state-error with respect to total consumption. This has the favorable property that it does not require labeled NTL data. In contrast, we evaluate a detector using Support Vector Machine (SVM) to detect NTL. Similar to the regression approach, the SVM classifies NTL based on the totalizer value as well as the state error at each point in time. In order to train the system, we artificially remove a subset of metered homes to synthesize NTL when training the model. The SVM is then trained as a binary classifier (NTL or NTL-free) with a confidence based on the distance from the support vector. The amount of NTL can be inferred from the state-error as compared to the NTL-free state error. Since the state error tends to have a high variance that increases with higher totalizer power, a radial basis kernel function (RBF) is adopted to learn a non-linear decision boundary to improve accuracy. A standard SVM optimization problem and the RBF kernel function $K(x, y)$ is given by

$$\begin{aligned} \min_{w,\xi,b} \quad & \frac{1}{2}w^T w + C\sum_{i=1}^{l}\xi_i \\ \text{subject to} \quad & y_i(w^T\phi(x_i) + b) \geq 1 - \xi_i, \\ & \xi_i \geq 0 \end{aligned}$$

$$K(x, y) \equiv \phi(x)^T\phi(y) = \exp(-\gamma||x - y||^2), \quad \gamma > 0$$

where x_i is the training vector which contains the value of totalizer and state error, ϕ is a function that maps variables x_i to a higher dimension, C is the penalty parameter of error estimations, and γ is the kernel parameter that is used to replace the dot product term in order to find non-linear boundaries. In order to prevent over fitting, the parameters C and γ are carefully selected through grid search and 10-fold cross validation during the training phase. The output of the SVM is a binary classification where given a totalizer value and a state error value it will determine if there is NTL or not. The amount of NTL can be determined based off of the state error and the distance from the support vector. There is a trade-off between how aggressive the SVM performs in terms of detecting low levels of loss and the number of false positives. When training the SVM, it is possible to adjust the threshold for what is

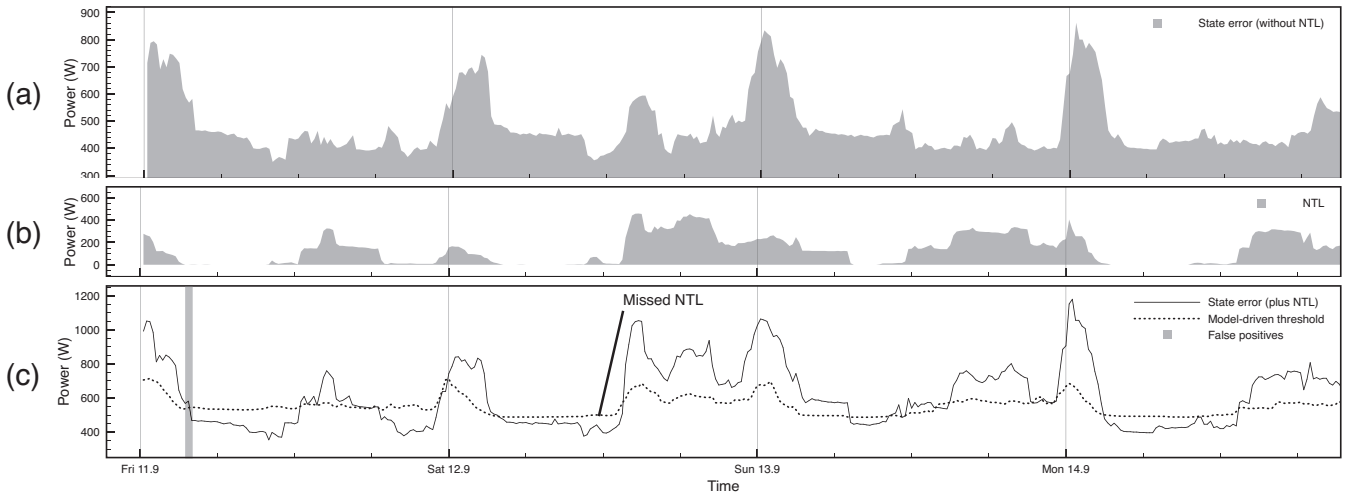

Figure 10: Example time-series showing (a) state error, (b) NTL, and (c) the state error containing NTL surpassing the detection threshold and triggering NTL detection

classifed as NTL in order to make the detector more or less conservative. In practice, we iteratively raise the NTL threshold in the training data until there are no false positives. This makes for a conservative detector, but one that will not constantly alarm grid operators.

6. EXPERIMENTAL EVALUATION

In this section, we experimentally evaluate implementations of the model-driven, regression-based, and SVM-based NTL detectors. Our evaluations employ a data-set containing 8 weeks of meter data from 525 households, collected at a 15-minute period. Each meter readings contains information pertaining to voltage, current, frequency, true power, power factor, meter state, uptime, as well as time-keeping and customer-related data. Totalizers are based on the same hardware as household meters and transmit the same information back to the network gateway. At the time of this work, certain parts of the microgrid were not yet outfitted with totalizers, thus our experiments focus on the 130 households in the "downtown" subdivision which are accounted for by a totalizer. The combined power consumption of the 130 households generally varies between 500 Watts and 1500 Watts, occasionally reaching peaks of over 2500 Watts.

Each detection approach was evaluated based on the the same 8-week data-set, with the first 4 weeks used as the training set and the next 4 weeks as the test set. Realistic NTL levels were simulated by leaving randomly selected meters out of the customer group and treating their consumption as NTL. This method is advantageous because it relies on real-world traces of consumption and it accurately simulates the side-effect of increased NTL, such as increased line losses. Figure 10 illustrates how (a) raw state error is combined with (b) NTL to form the state error as seen by (c) the generic detector. Any point in time at which the state error rises above the threshold is interpreted as the detection of NTL. One can observe an instance of NTL not being successfully detected and also an erroneous detection at a time of no NTL.

As stated earlier, the model-driven detector threshold is defined by $d_m(t) = m + l(t) + u$. In our evaluations of the model-driven detector, m has a value of 260 W to account for 130 meters with 2 Watt average power consumption, *l(t)* is computed using Gridlab-D, and u is assigned a value of 30 W as a buffer against noise. The resulting detector has a true positive rate over 97% for instances of NTL over 40 W, where the true positive rate is the percentage of occurrences of NTL successfully detected. The detector also has an overall true negative rate of 98.7%, where the true negative rate is the percentage of occurrences lacking NTL that are correctly identified. For the regression-based detector, we have defined the threshold as $d_r(P) = a * e^{b*P} + c$. After calculating the exponential regression using the first

	Amount of NTL (Watts)					
	0	1-20	20-40	40-60	60-80	80-100
Model	98.7%	6.4%	57.6%	97.9%	100%	100%
Reg.	99.5%	5.1%	59.0%	94.8%	91.1%	94.6%
SVM	100%	5.7%	51.2%	96.9%	99.4%	99.9%

Table 1: True negative rates and true positive rates between model-driven, regression, and SVM approaches, given different levels of NTL

	Amount of NTL (Watts)					
	0	1-20	20-40	40-60	60-80	80-100
7-day	98.3	10.5%	64.9%	94.0%	91.1%	94.6%
3-day	99.2	7.3%	58.7%	93.2%	91.1%	94.6%
1-day	99.7%	2.7%	59.0%	84.8%	91.1%	94.6%

Table 2: True negative rates and true positive rates of regression-based approach with respect to training duration, given different levels of NTL

	Amount of NTL (Watts)					
	0	1-20	20-40	40-60	60-80	80-100
7-day	100%	1.1%	23.6%	92.8%	99.4%	99.4%
3-day	100%	1.1%	18.6%	85.4%	99.2%	99.3%
1-day	99.9%	3.9%	29.8%	83.8%	99.1%	99.2%

Table 3: True negative rates and true positive rates of SVM approach with respect to training duration, given different levels of NTL

4 weeks of the data-set as the learning period, we find the relationship between totalizer power and detector threshold to be $a = 261.5, b = 1.5 * 10^{-4}, c = 34.2$. The resulting detector has a true positive rate over 90% for instances of NTL over 40 W, and an overall true negative rate of 99.5%. Lastly, the SVM-based detector is evaluated, using the same training and testing data-set as the previous two approaches. It is found to have a true positive rate of over 96% for instances of NTL over 40 W, and an overall true negative rate of 100%.

More detailed detection results can be found in Table 1, which compares the detection rates of the three approaches given different levels of NTL. Column *0* contains the true negative rate of each approach, while the rest of the columns represent the true positive rates of their respective bins. For example, the cell in the first row and fourth column indicates that for instances of NTL measuring between 40 W and 60 W the model-driven approach has a true positive rate of 97.9%. Of note here is the fact that all methods detect more accurately as the level of NTL is increased, with the model-driven and SVM approaches performing marginally better than the regression-based approach. In addition, the results suggest that the model-driven approached is slightly biased towards detecting smaller values of NTL, while the SVM-based approach has been successfully biased towards avoiding false positives.

Lastly, we explored the impact of the training period duration on the data-driven approaches' ability to detect NTL. Table 2 contains the true negative rates and true positive rates of the regression-based approach, given a small training period and different levels of NTL. Table 3 contains the same information for the SVM approach. The binning of data points in both tables is structured identically to the binning in Table 1. Surprisingly, we find that in both cases even one day of training is enough to achieve performance comparable to that of a 4-week training period. One explanation for this is that, after more than a year of operation, the Les Anglais microgrid has reached a steady state that does necessitate a long training period. Further data collection and analysis will be required to verify whether this holds true over the long term.

7. CONCLUSIONS

In conclusion, this paper presents a case study that evaluates how multiple forms of modeling in conjunction with synchronous sampling can be used to estimate the NTL within a microgrid. We show that line loss, sampling jitter and sensing error contribute significantly to the noise present in a metering system. We propose two classes of NTL detectors that look at state error, which is defined as the difference between totalizers typically located at generators and the sum of all of the meters in a microgrid. By both modeling and reducing (with synchronous sampling) the various sources of grid state error we are able to reliably detect NTL on the order of 1.6% (40W out of 2.5kW load) on a 525-household microgrid with a false positive rate lower than 2%.

We show how a detailed grid simulation using optimal power flow modeling on GPS mapped sources compares to two data-driven approaches. The first data-driven approach constructs a regression model based on a period of grid operation that is assumed to be NTL-free. This would ideally be captured shortly after a grid is installed. The second approach trains a binary SVM classifier based on synthetic NTL data generated by leaving a random subset of meters out of the aggregate power expression when computing state error. In general, we see that all of the approaches are quite similar, but the data-driven approaches require significantly less configuration data, making them easier to correctly implement. On the other hand, the data-driven approaches only classify NTL and provide less information about how the grid is performing. Detailed grid models have the benefit of being able to help optimize grid operations and plan the placement of new customers and sources of generation.

We believe that our approaches provide a valuable tool for grid operators and we are continuing to investigate mechanisms that learn system parameters at runtime to decrease the error detection tolerances. In the future, we intend to investigate localizing NTL through multiple distributed aggregators and by analyzing individual household trends.

8. REFERENCES

[1] World Bank Group, http://wdi.worldbank.org/table/5.11 (viewed 7/20/2015).

[2] Besant-Jones. Reforming power markets in developing countries: What have we learned. 2006.

[3] Mini-Grid Design Manual. Esmap technical paper 007. *Energy Sector Management Assistance Programme (ESMAP) UNDP/World Bank–April*, 2000.

[4] M. Buevich, D. Schnitzer, T. Escalada, A. Jacquiau-Chamski, and A. Rowe. Fine-grained remote monitoring, control and pre-paid electrical service in rural microgrids. In *Information Processing in Sensor Networks, IPSN-14 Proceedings of the 13th International Symposium on*, pages 1–11, April 2014.

[5] DESI Power:http://www.desipower.com/downloads/DESI-Power-Company-Profile.pdf.

[6] Chaudhuri. Renewable energy in the sundarbans. *New Delhi: The Energy and Resources Institute*, 2009.

[7] UNDP. Case studies of sustainable development in practice: Triple wins for sustainable development. *United Nations Development Program*, 2012.

[8] Kammen D Kirubi C, Jacobson A and A Mills. Community-based electric micro-grids can contribute to rural development: Evidence from kenya. *World Development 37:1208£1221.*, 2009.

[9] Devergy: http://www.devergy.com (viewed 10/10/2013).

[10] Circutor 2012a. Renewable Energies: http://circutor.com (viewed 2/22/2013).

[11] INENSUS: http://www.inensus.com/en/products5.htm (viewed 10/10/2013).

[12] Power Hive: http://powerhive.com (viewed 10/10/2013).

[13] GRAM Power: http://www.grampower.com/ (viewed 10/10/2013).

[14] Conlog http://www.conlog.co.za/pages/ProductsServices/Single-Phase-Meters.html (viewed 10/10/2013).

[15] Meg Harper. Review of strategies and technologies for demand–side management on isolated mini–grids. 2013.

[16] M. Khan and M. Iqbal. Pre-feasibility study of stand-alone hybrid energy systems for applications in newfoundland. *Renewable Energy*, 2005.

[17] Singh SP Rana S., Chandra R. and MS Sodha. Optimal mix of renewable energy resources to meet the electrical energy demand in villages of madhya pradesh. *Energy Conversion and Management*, 1998.

[18] Daniel M Kammen and Christian E Casillas. The delivery of low-cost, low-carbon rural energy services. 2011.

[19] TG Quetchenbach, MJ Harper, J Robinson IV, KK Hervin, NA Chase, C Dorji, and AE Jacobson. The gridshare solution: a smart grid approach to improve service provision on a renewable energy mini-grid in bhutan. *Environmental Research Letters*, 8(1):014018, 2013.

[20] T. Smith. Electricity theft: a comparative analysis. *Energy Policy*, 2004.

[21] Soma Shekara Sreenadh Reddy Depuru. Electricity theft: Overview, issues, prevention and a smart meter based approach to control theft. *Energy Policy*, 2011.

[22] A.R. Devidas and M.V. Ramesh. Wireless smart grid design for monitoring and optimizing electric transmission in india. In *Fourth Internation Conference on Sensor Technologies and Applications*, 2010.

[23] S. Salinas, C. Luo, W. Liao, and P. Li. State estimation for energy theft detection in microgrids. 2014.

[24] S.S.S.R. Depuru, Lingfeng Wang, and V. Devabhaktuni. Support vector machine based data classification for detection of electricity theft. In *Power Systems Conference and Exposition (PSCE), 2011 IEEE/PES*, pages 1–8, March 2011.

[25] J. Nagi, K.S. Yap, S.K. Tiong, S.K. Ahmed, and A.M. Mohammad. Detection of abnormalities and electricity theft using genetic support vector machines. In *TENCON 2008 - 2008 IEEE Region 10 Conference*, pages 1–6, Nov 2008.

[26] S. McLaughlin, B. Holbert, S. Zonouz, and R. Berthier. Amids: A multi-sensor energy theft detection framework for advanced metering infrastructures. In *Smart Grid Communications (SmartGridComm), 2012 IEEE Third International Conference on*, pages 354–359, Nov 2012.

[27] The Impact Lab JPS Project: http://theimpactlab.co/uncategorized/jamaica/.